Biomedical Optics EXPRESS

Ex vivo 4D visualization of aortic valve dynamics in a murine model with optical coherence tomography

Christian Schnabel,[1,3,*] Anett Jannasch,[2,3] Saskia Faak,[1,2,3] Thomas Waldow,[2] and Edmund Koch[1]

[1] *Technische Universität Dresden, Faculty of Medicine CGC, Department of Anesthesiology and Intensive Care Medicine and Clinical Sensoring and Monitoring, Germany*
[2] *Technische Universität Dresden, Faculty of Medicine CGC, Clinic for Cardiac Surgery, Germany*
[3] *Authors contributed equally to this paper*
** christian.schnabel@tu-dresden.de*

Abstract: The heart and its mechanical components, especially the heart valves and leaflets, are under enormous strain and undergo fatigue, which impinge upon cardiac output. The knowledge about changes of the dynamic behavior and the possibility of early stage diagnosis could lead to the development of new treatment strategies. Animal models are suited for the development and evaluation of new experimental approaches and therefor innovative imaging techniques are necessary. In this study, we present the time resolved visualization of healthy and calcified aortic valves in an ex vivo artificially stimulated heart model with 4D optical coherence tomography and high-speed video microscopy.

OCIS codes: (170.4500) Optical coherence tomography; (170.3010) Image reconstruction techniques; (000.1430) Biology and medicine; (170.6935) Tissue characterization; (170.3880) Medical and biological imaging; (170.2655) Functional monitoring and imaging.

References and links

1. S. H. Sündermann, D. Reser, M. Czerny, and V. Falk, "[Indication and timing of heart valve surgery - summery of the European guidelines]," Praxis (Bern 1994) **103**(8), 445–451 (2014).
2. N. M. Rajamannan, F. J. Evans, E. Aikawa, K. J. Grande-Allen, L. L. Demer, D. D. Heistad, C. A. Simmons, K. S. Masters, P. Mathieu, K. D. O'Brien, F. J. Schoen, D. A. Towler, A. P. Yoganathan, and C. M. Otto, "Calcific aortic valve disease: not simply a degenerative process: A review and agenda for research from the National Heart and Lung and Blood Institute Aortic Stenosis Working Group. Executive summary: Calcific aortic valve disease-2011 update," Circulation **124**(16), 1783–1791 (2011).
3. K. L. Sider, M. C. Blaser, and C. A. Simmons, "Animal models of calcific aortic valve disease," Int. J. Inflam. **2011**, 364310 (2011).
4. A. Alexopoulos, A. Kaoukis, H. Papadaki, and V. Pyrgakis, "Pathophysiologic mechanisms of calcific aortic stenosis," Ther. Adv. Cardiovasc. Dis. **6**(2), 71–80 (2012).
5. R. L. Osnabrugge, D. Mylotte, S. J. Head, N. M. Van Mieghem, V. T. Nkomo, C. M. LeReun, A. J. Bogers, N. Piazza, and A. P. Kappetein, "Aortic stenosis in the elderly: disease prevalence and number of candidates for transcatheter aortic valve replacement: a meta-analysis and modeling study," J. Am. Coll. Cardiol. **62**(11), 1002–1012 (2013).
6. T. Pilgrim and P. Wenaweser, "Aortic valve replacement in elderly with severe calcific aortic stenosis," Cardiovascular Medicine **13**, 197–203 (2010).
7. J. H. Chen, C. Y. Yip, E. D. Sone, and C. A. Simmons, "Identification and characterization of aortic valve mesenchymal progenitor cells with robust osteogenic calcification potential," Am. J. Pathol. **174**(3), 1109–1119 (2009).
8. M. Cimini, K. A. Rogers, and D. R. Boughner, "Smoothelin-positive cells in human and porcine semilunar valves," Histochem. Cell Biol. **120**(4), 307–317 (2003).
9. N. Latif, P. Sarathchandra, A. H. Chester, and M. H. Yacoub, "Expression of smooth muscle cell markers and co-activators in calcified aortic valves," Eur. Heart J. (2014).
10. R. H. Messier, Jr., B. L. Bass, H. M. Aly, J. L. Jones, P. W. Domkowski, R. B. Wallace, and R. A. Hopkins, "Dual structural and functional phenotypes of the porcine aortic valve interstitial population: characteristics of the leaflet myofibroblast," J. Surg. Res. **57**(1), 1–21 (1994).

#223204 - $15.00 USD Received 16 Sep 2014; revised 24 Oct 2014; accepted 24 Oct 2014; published 7 Nov 2014

11. M. Pho, W. Lee, D. R. Watt, C. Laschinger, C. A. Simmons, and C. A. McCulloch, "Cofilin is a marker of myofibroblast differentiation in cells from porcine aortic cardiac valves," Am. J. Physiol. Heart Circ. Physiol. **294**(4), H1767–H1778 (2008).
12. J. H. Chen and C. A. Simmons, "Cell-matrix interactions in the pathobiology of calcific aortic valve disease: critical roles for matricellular, matricrine, and matrix mechanics cues," Circ. Res. **108**(12), 1510–1524 (2011).
13. J. A. Leopold, "Cellular mechanisms of aortic valve calcification," Circ. Cardiovasc. Interv. **5**(4), 605–614 (2012).
14. K. Wyss, C. Y. Yip, Z. Mirzaei, X. Jin, J. H. Chen, and C. A. Simmons, "The elastic properties of valve interstitial cells undergoing pathological differentiation," J. Biomech. **45**(5), 882–887 (2012).
15. R. B. Hinton and K. E. Yutzey, "Heart valve structure and function in development and disease," Annu. Rev. Physiol. **73**(1), 29–46 (2011).
16. S. E. New and E. Aikawa, "Molecular imaging insights into early inflammatory stages of arterial and aortic valve calcification," Circ. Res. **108**(11), 1381–1391 (2011).
17. E. Aikawa, P. Whittaker, M. Farber, K. Mendelson, R. F. Padera, M. Aikawa, and F. J. Schoen, "Human semilunar cardiac valve remodeling by activated cells from fetus to adult: implications for postnatal adaptation, pathology, and tissue engineering," Circulation **113**(10), 1344–1352 (2006).
18. E. Aikawa, M. Nahrendorf, J. L. Figueiredo, F. K. Swirski, T. Shtatland, R. H. Kohler, F. A. Jaffer, M. Aikawa, and R. Weissleder, "Osteogenesis associates with inflammation in early-stage atherosclerosis evaluated by molecular imaging in vivo," Circulation **116**(24), 2841–2850 (2007).
19. E. Aikawa, M. Nahrendorf, D. Sosnovik, V. M. Lok, F. A. Jaffer, M. Aikawa, and R. Weissleder, "Multimodality molecular imaging identifies proteolytic and osteogenic activities in early aortic valve disease," Circulation **115**(3), 377–386 (2007).
20. R. B. Hinton, Jr., C. M. Alfieri, S. A. Witt, B. J. Glascock, P. R. Khoury, D. W. Benson, and K. E. Yutzey, "Mouse heart valve structure and function: echocardiographic and morphometric analyses from the fetus through the aged adult," Am. J. Physiol. Heart Circ. Physiol. **294**(6), H2480–H2488 (2008).
21. S. Bhat, I. V. Larina, K. V. Larin, M. E. Dickinson, and M. Liebling, "4D reconstruction of the beating embryonic heart from two orthogonal sets of parallel optical coherence tomography slice-sequences," IEEE Trans. Med. Imaging **32**(3), 578–588 (2013).
22. M. W. Jenkins, O. Q. Chughtai, A. N. Basavanhally, M. Watanabe, and A. M. Rollins, "In vivo gated 4D imaging of the embryonic heart using optical coherence tomography," J. Biomed. Opt. **12**(3), 030505 (2007).
23. M. W. Jenkins, F. Rothenberg, D. Roy, V. P. Nikolski, Z. Hu, M. Watanabe, D. L. Wilson, I. R. Efimov, and A. M. Rollins, "4D embryonic cardiography using gated optical coherence tomography," Opt. Express **14**(2), 736–748 (2006).
24. A. Mariampillai, B. A. Standish, N. R. Munce, C. Randall, G. Liu, J. Y. Jiang, A. E. Cable, I. A. Vitkin, and V. X. Yang, "Doppler optical cardiogram gated 2D color flow imaging at 1000 fps and 4D in vivo visualization of embryonic heart at 45 fps on a swept source OCT system," Opt. Express **15**(4), 1627–1638 (2007).
25. C. Schnabel, M. Gaertner, L. Kirsten, S. Meissner, and E. Koch, "Total liquid ventilation: a new approach to improve 3D OCT image quality of alveolar structures in lung tissue," Opt. Express **21**(26), 31782–31788 (2013).
26. S. Meissner, L. Knels, and E. Koch, "Improved three-dimensional Fourier domain optical coherence tomography by index matching in alveolar structures," J. Biomed. Opt. **14**(6), 064037 (2009).
27. L. Kirsten, M. Gaertner, C. Schnabel, S. Meissner, and E. Koch, "Four-dimensional imaging of murine subpleural alveoli using high-speed optical coherence tomography," J. Biophotonics **6**(2), 148–152 (2013).

1. Introduction

Calcific aortic valve stenosis (AVS) is the most common heart valve disease in North America and Europe [1] and shares many risk factors with atherosclerosis such as older age, male gender, hypercholesterolemia, hypertension, smoking and metabolic syndrome [2,3]. AVS is a significant public health problem and a major cause of morbidity and mortality in elderly adults as it affects 2.5% of people over 65 years of age [4]. The prevalence in the elderly over 75 years of age is 12.4%, which corresponds to 4.9 million patients in the European countries [5]. Considering the demographic change, the prevalence of aortic heart valve disease will significantly rise as for the year 2015 the predicted part of the population ≥ 65 years in Europe, Switzerland, Japan and North America for the formation of AVS is 35% [6].

During the more than three billion heart beats over the average person's lifetime, the aortic valve operates in an extreme hemodynamic environment. The aortic valve is composed of three semilunar cusps, which maintain unidirectional blood flow from the left ventricle into the aorta during the cardiac cycle. The residing cells are represented by endothelial and interstitial cells, a heterogeneous population of fibroblasts in a quiescent state, a smaller population of mesenchymal progenitor cells [7], smooth muscle cells and myofibroblasts [8–

#223204 - $15.00 USD Received 16 Sep 2014; revised 24 Oct 2014; accepted 24 Oct 2014; published 7 Nov 2014

11]. These cells secrete and build components of the extracellular matrix like collagen, elastin and glycosaminoglycanes and are therefore responsible for composition, elasticity and cohesiveness of the valve cusps [12–14]. The aortic valve is subjected to three basic loading states – flexure, shear and tension [2,15], which may influence valve remodeling or pathological changes. Until now, little is known about the pathogenesis and progression of AVS because the clinical manifestation of the disease is preceded by a mostly undetected multi-year process of inflammation and fibrotic changes leading to thickened and stiff valve cusps with decreased flexibility and left ventricular outflow obstruction. Compensatory mechanisms drive heart muscle hypertrophy and the disease becomes symptomatic [15]. At this point, untreated AVS becomes fatal in an average of 5 years. To date, pharmacological therapies that can stop or reverse the pathogenesis of AVS are not available. Hence, the surgical replacement of the aortic valve, with either mechanical or biological valve prostheses, is the only curative treatment affecting annually 275,000 patients worldwide [16].

Aortic valve disease manifests as stenosis and/or regurgitation and is characterized by a massive fibrotic disorganization of the extracellular matrix as well as alterations in the residing cell populations. In the case of AVS due to collagen production and elastin fragmentation, the elasticity of the valve tissue decreases and physiologically quiescent fibroblasts, like valvular interstitial cells (VICs), become activated. As a possible initiating event, the disruption of the endothelial layer through alterations in the blood-stream-driven shear stress is discussed [17]. Although the molecular and physiological regulators, which causally trigger and control differentiating events towards VICs, are not clear, it is known that alterations in the mechanobiological properties towards increased stiffness promote pathological cellular processes building a vicious circle within the development of AVS [13]. Further progression leads to calcification with still preserved normal valve function and is referred to as aortic valve sclerosis, a characteristic of the progressing disease [2,3]. In advanced cases further calcification and thickening of the cusps forwards further impairment of valve opening.

Animal models provide a powerful tool to study valve biomechanics as well as the progression of AVS. Beside rabbit and swine, mouse is the most common species used [15]. Although mechanics of murine valves are difficult to test due to their small size, mouse models offer the advantages to demonstrate the progression of AVS within short timeframes and feature significant benefit providing genetic knockouts [15]. Under high fat/high cholesterol diet, $ApoE^{-/-}$ mice develop hyperlipidemia, thickened cusps, activated endothelial cells and subendothelial lesions [18,19] and represent an excellent tool to investigate potential key molecular modulators of heart valve disease [15].

Currently, echocardiography is a useful tool for monitoring AVS in humans and mice [20]. It enables the visualization of aortic valve anatomy, the detection and quantification of hemodynamic obstruction as well as measurements of transvalvular blood flow velocity, mean pressure gradient and computation of valve area. Although useful for visualization of the valves' biomechanical properties, distinguishing a bicuspid from a normally developed valve with three cusps via echocardiography can be challenging. Furthermore, the low spatial resolution does not allow the detection and quantification of early stage thickening due to calcification deposit and therefore is less applicable for monitoring early stage of AVS.

One of the recommendations for future research on AVS by The National Heart, Lung and Blood Institute Aortic Stenosis Working Group includes the development of high-resolution imaging modalities for the identification of subclinical AVS [2]. Therefore, we present a novel approach for the characterization of biomechanical properties of murine aortic heart valves by using optical coherence tomography (OCT) and high-speed video microscopy in an *ex vivo* murine heart model. The objective of this study is to show the feasibility of these imaging techniques to visualize aortic valve during uninterrupted artificial stimulation. 4D OCT was previously performed by several groups using gating techniques and high-speed OCT systems to visualize the murine heart [21–24]. The advantage of the presented imaging

#223204 - $15.00 USD Received 16 Sep 2014; revised 24 Oct 2014; accepted 24 Oct 2014; published 7 Nov 2014

techniques is the high temporal and spatial resolution in 2D for video microscopy and 3D for OCT by using a low-speed OCT system. The aim of further studies is to characterize the dynamic properties and to compare the measurements of clinically relevant dynamic parameters of the valves with respect to different pathological conditions. This will allow identifying early stage of the disease before significant hemodynamic obstruction has occurred and cannot be reversed.

2. Methodology

2.1 Ex vivo heart preparation

All experiments were approved by the animal care and use committee of the local government authorities and were performed in accordance with the Guide for Care and Use of Laboratory Animals (Institute of Laboratory Animal Resources, 7th edition, 1996). In this study, ten 17-week-old C57BL/6J wildtype and seven 12-month-old ApoE knockout mice on C57BL/6J background were used. For this first study the old ApoE knockout mice were contributed by a cooperating group. So at this stage, a detailed characterization of the calcification of the valves with histology was not available, but will be done in further progress of the work. The ApoE knockout mouse is an established model for the investigation of heart valve diseases and histopathological analyses were carried out by several groups [18,19]. Therefore, we compared the tissue structure using microscopic observation and the differences in tissue thickness in OCT cross-sections (compare to Fig. 3 and 4) as evidence of the disease progression.

The mice were anesthetized with an intraperitoneal injection of ketamine/xylazine (120 mg/kg/bodyweight and 8 mg/kg/bodyweight) and heparinized (500 I.U./25 g bodyweight). Afterwards, they were sacrificed by cervical dislocation and the hearts were removed immediately and rinsed in PBS to remove the entire blood. The aorta was shortened as much as possible to assure an optimal view of the OCT scanner head onto the aortic valve cusps. Successful visualization of the aortic valve through the intact aortic wall with the used OCT setup was not possible in this preliminary study. Finally, the apex of the heart was cut off and a catheter was inserted into the left ventricular outflow tract to mimic the normal flow direction through the aortic valve with a custom-made pump. The heart was fixed onto the catheter by a nylon suture to prevent sliding off due to the induced pressure during artificial stimulation of the valve.

2.2 Experimental setup and artificial stimulation of aortic valves

This study targets dynamic visualization of murine aortic valves with optical coherence tomography. As we found no suitable established heart model for dynamic visualization, we created an experimental setup shown in Fig. 1, consisting of a custom-made pump for artificial stimulation of the aortic valve controlled by custom-made software and the imaging system for OCT and video microscopy. The device is a modified version of an experimental small animal ventilator [25] and consists of two independent syringe pumps, one to insert and one to withdraw fluid (PBS), and two pinch valves for controlling the flow direction. Stimulation is pressure-controlled following a sinusoidal pattern. Pressure limits were adjusted individually to each heart in such a way that the pumped volume of each cycle is approximately 40 µl to mimic the normal stroke volume through the valve. The normal heart rate is about 600 bpm, so physiological flow cannot be simulated with this setup. But by imitating at least the physiological stroke volume, the tissue strain and movement is similar and allows the visualization of the different valve dynamics and the comparability of the measurements for both, healthy and diseased tissue. Due to the open heart model, the fluid pumped through the valve flows into the preparation chamber and is recirculated to the reservoir. To mimic the closing of the valve due to the blood volume in the aorta, one of the two pumps withdraws fluid from the heart until the pressure matches the lower pressure limit.

#223204 - $15.00 USD Received 16 Sep 2014; revised 24 Oct 2014; accepted 24 Oct 2014; published 7 Nov 2014

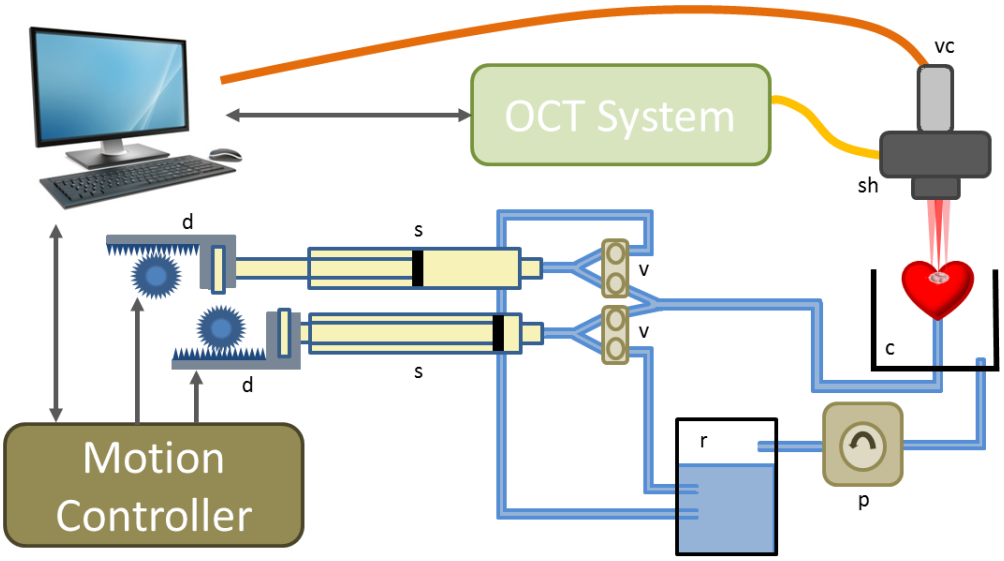

Fig. 1. Experimental setup for 4D visualization of aortic valves in mice. The setup consists of two independent pumps to perform the opening and closing of the aortic valve during artificial stimulation. The fluid bolus coming through the valve during each cycle is recirculated to a reservoir by a peristaltic pump. The scanner head enables the simultaneous acquisition of the aortic valve with 3D OCT and high-speed video microscopy. Components: vc... high-speed video camera; sh…OCT scanner head; c… heart chamber; p… peristaltic pump; r… reservoir; v… valve; s… syringe; d… linear drive

This setup allows the simulation of heart beat frequencies up to 120 beats per minute (bpm) and different stimulation patterns can be chosen for further investigations. The frequency in this study was set to 50 bpm to reduce motion artifacts and to increase temporal resolution for OCT imaging.

2.3 Imaging system and image acquisition

A spectral domain OCT system [26] with a center wavelength of 830 nm and a band width of 50 nm at half maximum was used with an A-scan rate of 12 kHz to visualize the structure and dynamics of the aortic valves *ex vivo*. The system allows the simultaneous acquisition of 3D OCT and 2D microscopy images by using the same beam path. For OCT, the near-infrared light from a superluminescence diode (Superlum, Russia) is guided to the scanner head containing a Michelson interferometer. The incoming light is separated by a beam splitter into a sample beam and a reference beam, which is deflected by a mirror. The sample beam can be deflected by two galvanometer scanners (Cambridge Technology Inc., USA) in x and y direction to perform a scan pattern over the sample. The backscattered and reflected light from different sample depth is guided back to the beam splitter and superimposed with the reference beam. This interference signal is spectrally resolved by a diffraction grating and measured by a line-detector (Teledyne DALSA Inc., Canada). The depth dependent information is calculated by a Fast Fourier Transformation and the logarithm of the intensity is displayed on an 8 bit gray scale. Therefore, the whole depth dependent information can be acquired with one single shot called A-scan.

To acquire a 2D image of a sample, one galvanometer scanner (x) is rotated to measure adjacent A-scans resulting in cross-sectional images (B-scan). By deflecting the second galvanometer scanner (y), adjacent B-scans can be acquired forming the 3D OCT image.

As the OCT system is not fast enough to acquire 3D images of the moving aortic valve, a scanning algorithm making use of the repetitive tissue movement due to the artificial stimulation was applied. Therefore, the image acquisition of cross-sections is continuously

#223204 - $15.00 USD Received 16 Sep 2014; revised 24 Oct 2014; accepted 24 Oct 2014; published 7 Nov 2014

performed without interruptions at the same position by deflecting just the x-galvanometer scanner. A trigger signal created from the pump device after each stimulation cycle sets the position of the second galvanometer scanner one step further and again cross-sections are continuously acquired at this new position. The following example describes this continuous scanning algorithm as it was performed during this study.

The artificial heart beat was set to 50 beats per minute resulting in a cycle time of 1.2 s per beat. The image size of a single cross-section was set to 320 x 512 (b x h) Pixel and 320 adjacent cross-sections were used for a 3D image. The 12 kHz clock enables the acquisition of 320 A-scans in 30 ms, which is fast enough to avoid motion artifacts within single cross-sections and to visualize different motion states of the valves. To acquire 320 adjacent cross-sections for the 3D images with the algorithm described above, 320 heart beats have to be performed resulting in an overall measurement time of approximately 6.4 minutes. The achievable time resolution only depends on the number of A-scans in each cross-section with this scanning mode and is for this example 30 ms. Thus, 40 3D OCT image stacks show the dynamic movement of the aortic cusps.

To perform microscopic imaging with a high-speed camera (acA2000-340kc, Basler, Germany) at 50 fps, a dichroic mirror couples visible light into the same beam path used for OCT to obtain the same region of interest with both imaging techniques. The video sequence is acquired directly prior to the OCT measurement, because of the different measurement time and to avoid storage disturbance due to the high data transfer rates.

2.4 Image post processing

Due to the continuous image acquisition mode, the cross-sections have to be rearranged to create the 3D OCT images showing different states of the motion. Therefore, the first B-scans from all 320 cycles were resampled forming the first 3D OCT stack. This is done similarly for all following B-scans. The result of this rearrangement is the 4D visualization of the valve movement during artificial stimulation consisting of 40 3D image stacks.

3. Results

Images of murine aortic valves with both techniques, OCT and video microscopy, are shown in Fig. 2 under steady state conditions without artificial stimulation. While microscopy images only provide a 2D view of the structures, OCT achieves a real 3D visualization of the valvular cusps and surrounding morphology. In some cases deeper structures like the mitral leaflet (marked by m in Fig. 2) become visible depending on the heart size and preparation. The reason for the usage of an open heart model with removed aorta is also visible in Fig. 2. The imaging depth for OCT is limited due to the scattering loss in deeper tissue structures. But especially the residues of the aortic wall (see a1/a2 in Fig. 2) leads to a remarkable signal reduction, so OCT imaging through the intact vessel was not possible with this imaging setup (compare to the triangle marks in Figs. 2, 3, and 4).

#223204 - $15.00 USD Received 16 Sep 2014; revised 24 Oct 2014; accepted 24 Oct 2014; published 7 Nov 2014

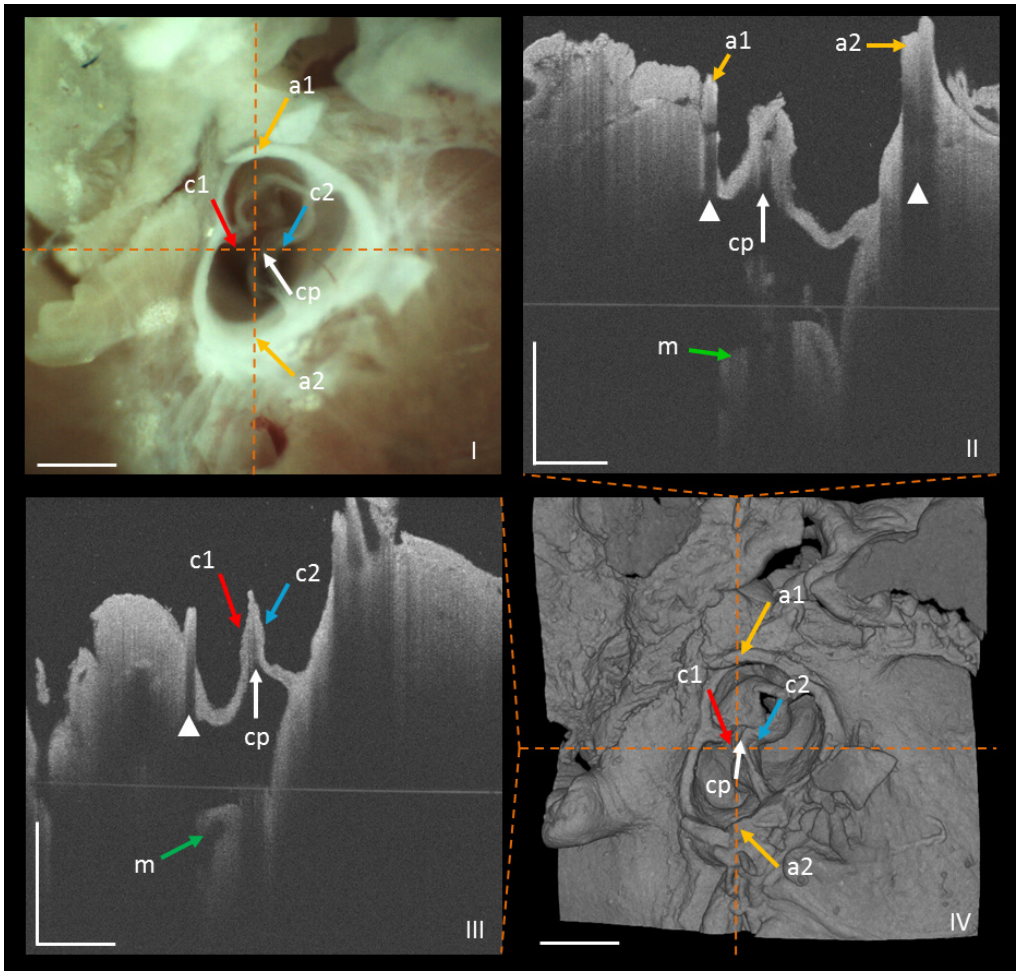

Fig. 2. Visualization of a murine aortic valve with 2D video microscopy (I) and 3D OCT (IV) *ex vivo*. These images were acquired after preparation of the aortic valve without any stimulation. The structures of the valve are clearly visible in both imaging techniques. The OCT cross-sections (II and III) show two closed cusps of the aortic valve and also a mitral valve leaflet beneath. Due to the tissue structure of the aorta, penetration depth for OCT is remarkably limited (see the loss of structure information at the annulus in the cross-sections marked by the triangles), which is the reason why an imaging through the intact aorta vessel was not feasible with this setup. Remarkable landmarks: a1 a2… aortic wall residues; c1 c2… aortic cusps; cp… coaptation point; m… mitral leaflet. Scale bar is 500 µm.

As described above, for dynamic measurements 40 3D OCT images were acquired showing the different states of the valve movement. To show the feasibility of imaging the aortic valve dynamics with video microscopy and OCT, we performed these measurements on female young healthy wildtype mice and older ApoE knockout mice. Exemplary findings are shown in Figs. 3 and 4 where the aortic valve of a 17-week-old C57BL/6J (Fig. 3) and a 12-month-old ApoE knockout mouse (Fig. 4) was visualized under same conditions of artificial stimulation. The images shown here are representative examples and were supported by ten measurements of 17-week-old wildtype and seven measurements of 12-month-old ApoE knockout mice showing the differences in the valvular structure and tissue movement due to the progression of heart valve disease. To highlight our findings, four exemplary states of the movement were chosen. Images of the closed and maximally opened valve are not hampered by motion artifacts and therefore image quality is good in spite of 6.4 minutes overall

#223204 - $15.00 USD Received 16 Sep 2014; revised 24 Oct 2014; accepted 24 Oct 2014; published 7 Nov 2014

measurement time and 320 different stimulation cycles. While images of the half opened and half closed valve were acquired during the fast movement of the sinusoidal stimulation, motion artifacts appear in single cross-sections, which leads to blurring effects (marked by the diamonds in Figs. 3 and 4). While all three cusps of the healthy young mouse open widely, opening movement of one cusp of the ApoE knockout mouse is terminated due to advanced calcification and AVS phenotype (see l1 in Fig. 4). Due to this late stage of the disease in the 12-month-old knockout mouse, the differences in the aortic structure are clearly visible between both mice regarding the thickness of the aortic tissue and the opening area of the valve. While these differences are difficult to see in the video microscopy images, OCT provides a clear insight into the tissue structure.

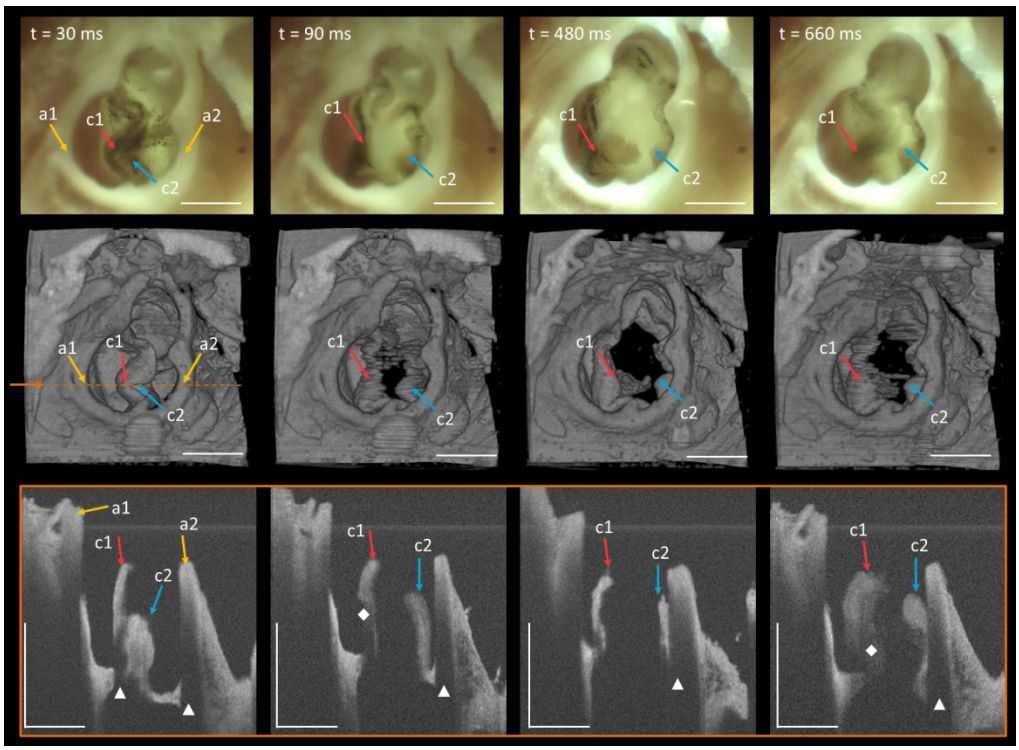

Fig. 3. The aortic valve of a female 17-week-old C57BL/6J mouse. The four images of each row are examples of the original series of 40 different OCT images of the dynamic measurement and show the closed, half opened, maximum opened and half closed state of the aortic valve during artificial stimulation with high-speed video microscopy (first row), enface OCT (second row) and OCT cross-sections (last row), respectively. Due to the long measurement time and the scanning algorithm, motion artifacts partly appear especially in the slope time of the sinusoidal stimulation pattern but nevertheless image quality is good enough to investigate dynamic behavior and properties of the valvular cusps. Orange arrow indicates the position of the cross-sections. Scale bar is 500 µm. (see first row in Media 1)

#223204 - $15.00 USD Received 16 Sep 2014; revised 24 Oct 2014; accepted 24 Oct 2014; published 7 Nov 2014

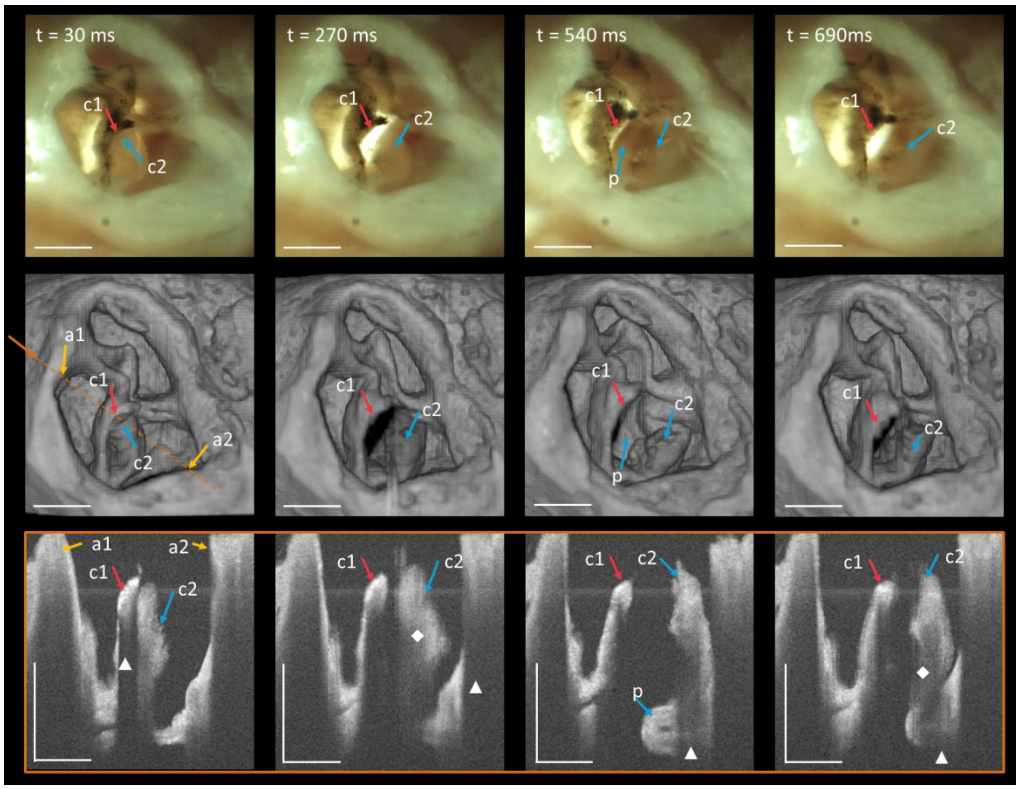

Fig. 4. Example images of the valve dynamics of a 12-month-old female ApoE knockout mouse. It is clearly visible that the aorta tissue is thickened compared to Fig. 3 and the motility of the cusps is decreased. Especially the left cusp is so stiff that it doesn't move during stimulation, which seriously restrains the hemodynamics of the blood flow. From the video images and OCT enface view the impression occurs that the valve opens just a very little area. But due to the 3D information provided by OCT, one can see that the cusps are folded and extend into the valves opening area (p). This is also based on the progressive calcification of the cusps annulus structure. Marks: a1, a2 … aortic wall residues; c1, c2**…** aortic cusps; p …plait of the right cusp. Orange arrow indicates the position of the cross-sections. Scale bar is 500 µm. (see second row in Media 1)

The angle of view differs between each heart and therefore it is difficult to compare the measurements and parameters with 2D imaging techniques. OCT enables the measurement and comparison of all parameters like maximum opening area due to the 3D image information. This can be obtained in the third column of Fig. 4. While video microscopy and OCT enface images show little opening of the valve, one can see in the cross-sectional view (third column) that the opening is much wider than it seems. Due to the movement, the plait (marked with p in Fig. 4) of the right cusp turns upwards and appears in the flow channel, which leads to the impression of a closed valve in the enface views. Therefore, the 3D image information from OCT is a useful tool for further detailed analysis of the dynamic behavior of aortic valve tissue.

As a consequence of progressive calcification, the loss of intensity for OCT is also increased and deeper structures disappear in the images. Nevertheless, thickness of the valvular tissue and information about dynamic properties like maximum opening area of the cusps can be measured from these images.

The main intension of this paper is to introduce new imaging techniques for the visualization of the aortic valve dynamics. Extensive histological and statistical measurements have to be performed in further steps but are beyond the scope of the present communication.

#223204 - $15.00 USD Received 16 Sep 2014; revised 24 Oct 2014; accepted 24 Oct 2014; published 7 Nov 2014

However, first measurements were realized on two samples (Fig. 3 and Fig. 4) regarding the maximum opening area and the motion characteristics of the cusps. Therefore, OCT enface projection was generated from the 3D images in such a way, that the flow channel is not hidden by other structures. These projections were used for manual segmentation of the valve opening area at dedicated timepoints shown by the 40 3D OCT images. To compare the 17-week-old wildtype and the 12-month-old ApoE knockout mouse, we also segmented the residual aortic tissue and measured the opening area as percentage of the residual aorta. The results are shown in Fig. 5. It becomes clearly visible that the healthy young wildtype valve opens wider and earlier compared to the diseased ApoE knockout valve. This seems to be in good agreement with the idea that stiffer and calcified tissue needs more pressure to open than the non-diseased motile valve tissue.

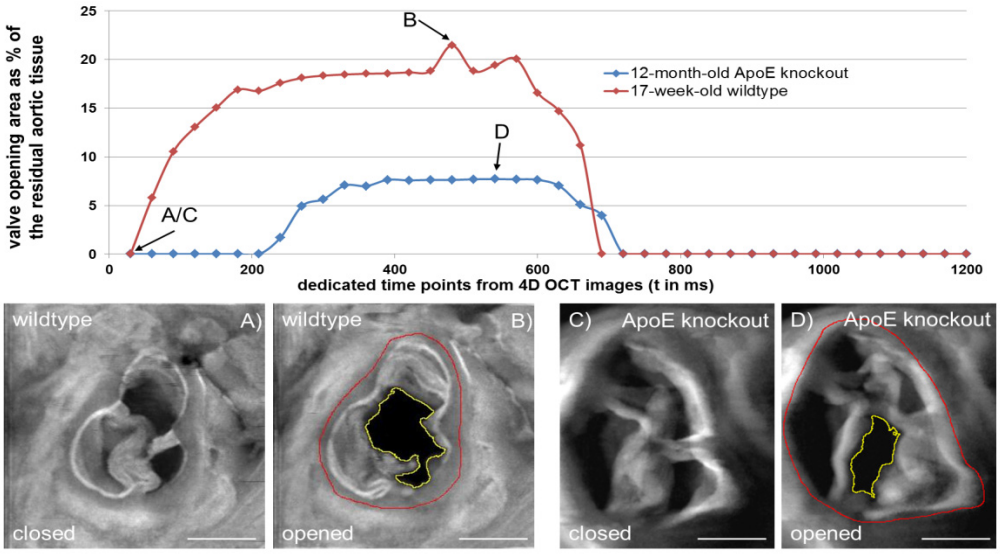

Fig. 5. Measurement of the valve opening area. OCT enface projection was used to manually segment the opening area of the healthy and diseased valves from Fig. 3 and Fig. 4, respectively (indicated by yellow line). This was done for each 3D OCT image. To compare these measurements the residual aortic tissue was also segmented as the reference value (indicated by red line). The opening area is displayed as percentage of these reference values for both valves in the upper plot. The diseased tissue is stiffer and therefore the valve opens later after the pressure gradient is higher caused by our pump. Furthermore, the maximum opening area is much smaller compared to the healthy tissue. Acquisition time points of images A, B, C and D are marked in the upper plot. Scale bar is 500 µm.

These are first preliminary results and further investigations have to address the segmentation of the exact flow channel profile to assure measurement results. Nevertheless, the overall trend of different dynamics between healthy and diseased aortic valves is clearly visible from these data.

4. Discussion and outlook

The presented results show that optical coherence tomography and high-speed video microscopy are promising tools for the investigation of dynamic behavior and its changes in calcific aortic valve stenosis disease models in mice. OCT offers an easy access to the tissue morphology in 3D and the measurement of tissue parameters like thickness without any sample preparation like staining or cutting. This first study of imaging aortic valve dynamics shows also some limitations of the used setup.

Due to long measurement time for the gated OCT data acquisition motion artifacts appear during the fast tissue movement. During less tissue movement the reconstruction algorithm

#223204 - $15.00 USD Received 16 Sep 2014; revised 24 Oct 2014; accepted 24 Oct 2014; published 7 Nov 2014

works very well and there is no jitter visible in the OCT cross-sections of the slow scanning axis (Fig. 6(a)). During the phase of high tissue acceleration and due to the measurement over several cycles, the cusps are not in exactly the same position from cycle to cycle and therefore jitter occurs in the slow axis cross-sectional view (compare to Fig. 5(b)). The maximum axial shift occurring in the reconstructed images was estimated with 96 µm in the fast moving tissue (see # in Fig. 6). Areas with slow moving tissue are less subjected to jitter (see * in Fig. 6).

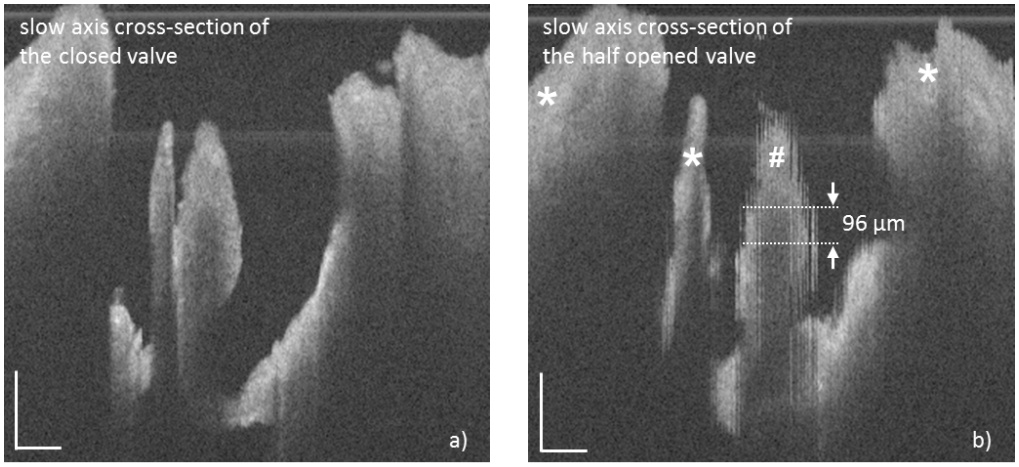

Fig. 6. Estimation of the axial shift between OCT B-scans due to motion artifacts. Due to the gating technique for OCT measurements, jitter between single B-scans occurs in the reconstructed 3D volume stack. This jitter can be seen in the slow scanning axis cross-sectional view. While the reconstruction works very well during phases of low tissue movement (a)), the fast acceleration of the cusps in addition to the measurement over several cycles yields little jitter and blurring effects (b)). The axial shift between B-scans was estimated from the images with 96 µm. Areas, which move slowly (marked with *) are less subjected to jitter than fast moving tissue (marked with #). Scale bar is 200 µm.

Because an established heart model was not available for this study, the valve structure was artificially stimulated by a custom-made liquid pump with a frequency of 50 bpm in a sinusoidal pattern, which is one order of magnitude lower than the physiological heartbeat of a mouse. The dynamics of the tissue is not only influenced by the viscosity of the liquid but also by the velocity itself. The influence of the rate change and the stimulation pattern on the tissue dynamics has to be investigated in further experiments. Furthermore, the motion of the cusps is also influenced by other compartments of the heart, and the aorta. Therefore, a working heart setup should be used to keep the aortic valve tissue environment and the tissue movement as realistic as possible and to overcome most of the limitations mentioned before.

To prove our findings and to compare it to more established techniques used for the investigation of aortic valve stenosis, histophatological analysis of each sample will be performed after the dynamic visualization with OCT and video microscopy in further studies. Furthermore, to evaluate the 4D OCT visualization and to prove further measurements, other noninvasive imaging techniques, showing the valve dynamics like ultrasound biomicroscopy, should be used. Until now, a suitable device is not available at this stage of our studies.

OCT can be a helpful tool to observe drug therapies and novel approaches for the treatment of AVS in animal models. The high spatial and temporal resolution enables new insights into the course of this disease and may lead to a characterization and identification of early stages before significant hemodynamic obstruction has occurred and intervention by novel drug therapies is possible. This first feasibility study reveals further steps to enhance the experimental setup and imaging techniques to increase the information content of the measurements and thereby rising comparability of the results to clinically relevant parameters

#223204 - $15.00 USD Received 16 Sep 2014; revised 24 Oct 2014; accepted 24 Oct 2014; published 7 Nov 2014

and results from other imaging techniques used for the investigation of murine AVS. Therefore, a high-speed FDML based OCT system [27], which enables A-scan rates of 240 kHz instead of 12 kHz used in this study and additionally OCT Doppler measurement for flow field analysis should be used, which also enables the prevention of motion artifacts in the images. Beside the usage of a high-speed OCT system, the gating technique can be improved e. g. based on the measurements of the heart motion phases in a working heart model or advanced gating techniques as described by other groups [21–24]. A challenging task will be the visualization of the cusps through the intact aortic vessel in spite of OCT signal reduction to use this imaging technique in a working heart model. Further studies on *ex vivo* and in vivo heart models using high-resolution and label-free imaging techniques like OCT can increase the understanding of essential processes of evolving aortic valve diseases and can help to develop new therapy strategies.

Acknowledgments

This project was financially supported by the Else Kröner-Fresenius-Stiftung.

#223204 - $15.00 USD Received 16 Sep 2014; revised 24 Oct 2014; accepted 24 Oct 2014; published 7 Nov 2014